PAPER

Vancomycin conjugated iron oxide nanoparticles for magnetic targeting and efficient capture of Gram-positive and Gram-negative bacteria

Mehnaz Rashid,[a] Md. Ahasanur Rabbi,[a] Tabassum Ara,[b] Md. Motahar Hossain,[a] Md. Shahidul Islam,[a] Abdelhamid Elaissari,[c] Hasan Ahmad [ID] *[a] and Md. Mahbubor Rahman [ID] *[a]

Drug conjugated iron oxide magnetite (Fe_3O_4) nanoparticles are of great interest in the field of biomedicine. In this study, vancomycin (Van) conjugated magnetite (Fe_3O_4) nanoparticles were envisioned to capture and inhibit the growth of bacteria. Hydrophobic Fe_3O_4 nanoparticles were synthesized by using co-precipitation of ferrous (Fe^{2+}) and ferric (Fe^{3+}) ions following a surface modification step with oleic acid as stabilizers. Thereafter, a ligand exchange technique was employed to displace oleic acid with hydrophilic dopamine (DOPA) molecules which have a catechol group for anchoring to the iron oxide surface to prepare water dispersible nanoparticles. The surface of the resulting Fe_3O_4/DOPA nanoparticles contains amino ($-NH_2$) groups that are conjugated with vancomycin *via* a coupling reaction between the $-NH_2$ group of dopamine and the $-COOH$ group of vancomycin. The prepared vancomycin conjugated Fe_3O_4/DOPA nanoparticles were named Fe_3O_4/DOPA/Van and exhibited a magnetic response to an external magnetic field due to the presence of magnetite Fe_3O_4 in the core. The Fe_3O_4/DOPA/Van nanoparticles showed bactericidal activity against both Gram positive *Bacillus subtilis* (*B. subtilis*) and *Streptococcus* and Gram-negative bacteria *Escherichia coli* (*E. coli*). Maximum inhibition zones of 22 mm, 19 mm and 18 mm were found against *B. subtilis*, *Streptococcus* and *E. coli* respectively. Most importantly, the vancomycin conjugated nanoparticles were effectively bound to the cell wall of the bacteria, promoting bacterial separation and growth inhibition. Therefore, the prepared Fe_3O_4/DOPA/Van nanoparticles can be promising for effective bacterial separation and killing in the dispersion media.

1. Introduction

Infections caused by drug resistant bacteria (also known as 'superbugs') in community places and hospitals have prompted growing concern all over the world.[1,2] Limited options remain for treating infections caused by such resistant bacteria. Vancomycin as an antibiotic has been used for treating bacterial infection for many years. This glycopeptide antibiotic binds to the terminal D-alanyl-D-alanine residues of lipid II and nascent peptidoglycan cell wall precursors, thus blocking the bacterial transglucosylases and transpeptidases required for peptidoglycan biosynthesis and cross-linking.[3,4] As the bacterial cell wall of Gram-positive bacteria is composed largely of peptidoglycan, vancomycin and the related glycopeptide antibiotics

prevent cell division and are bacteriostatic in action.[5] Despite of the potential for the retardation of bacterial growth, unfortunately, the use of free vancomycin is less efficient for site specific applications. The drug delivery *via* a vector to an infection site is more efficient as free drug distributes/diffuses randomly all over the body including the infection site.[6,7] The use of free drug also requires higher dose which may cause side effects and toxicity, needs to be reduced by using a carrier platform. In this respect, the antibiotics loaded on nanoparticles or into polymer matrix could be a promising approach for reducing toxicity, and side effects due to greater access and accumulation of the active molecules at the infection site.[8]

Iron oxide nanoparticles (IONPs) have attracted an extensive attention because of their potential applications in biomedical field for magnetic resonance imaging (MRI), magnetic hyperthermia, cancer therapy, drug delivery and biomolecule separation.[9–13] However, bare iron oxide nanoparticles have limitations that include colloidal instability, leaching out, toxicity, and degradation in biological medium.[14] Therefore, different efforts have been devoted for coating and surface modification of IONPs with different materials such as polymers, silica, and ligand molecules, dextran, and surfactants.[15,16]

[a] *Polymer Colloids & Nanomaterials (PCN) Group, Department of Chemistry, Faculty of Science, University of Rajshahi, Rajshahi 6205, Bangladesh. E-mail: samarhass@yahoo.com; mrchem@ru.ac.bd*

[b] *Department of Biochemistry and Molecular Biology, Faculty of Science, University of Rajshahi, Rajshahi 6205, Bangladesh*

[c] *Université Lyon, University Claude Bernard Lyon-1, CNRS, ISA-UMR 5280, Lyon F-69622, France*

Specifically, Nahar *et al.* reported poly(*N*-isopropyl acrylamide-co-acrylic acid) polymer coated IONPs for dual temperature and pH responsive magnetic nanocomposites synthesis.[17] In a recent work, Wang and his coworkers synthesized amphiphilic thermally sensitive block helical poly(phenyl isocyanide) polymer to prepare magnetic micelle complex for temperature-controlled drug delivery.[18] Polymer coating on IONPs also reduces the generation of reactive oxygen species (ROS) which may cause cellular degradation.[19] Besides, silica coating on IONPs has been promising because of its biocompatibility, and ease of further functionalization with other polymers, and molecules.[20,21] In addition to that, the surface of IONPs have also been modified with some other organic ligands, *e.g.*, catechol and phosphocholine group containing molecules, that have very high affinity to anchor with metal oxide nanoparticles' surface.[22] Dopamine has emerged great interest as capping agent for IONPs due to the stability and strength of the resultant five-membered metallocycle chelate and the ease at which it can be functionalized through amide bonds with other molecules of interest.[23–25]

The major advantages of drug loaded magnetic nanoparticles are easy accumulation and separation from a dispersion media by using an external magnet. Nonetheless, most of the literatures related to antibacterial IONPs reported mainly antibacterial property of nanoparticles. For example, Pimpha *et al.* recently reported the preparation of cationic polymer coated IONPs for antimicrobial activity.[26] Besides, antibacterial polyguanidine coated magnetite (Fe$_3$O$_4$) nanoparticles have been synthesized for antibacterial activity study against *E. coli*.[27] Lee *et al.* reported the development of an interesting technique to separate bacteria from blood using magnetic nanoparticles modified with synthetic ligand.[28] Likewise, magnetic nanoparticles coated with different polymers have also been reported for bacteria separation.[29,30] In addition to that, special attention for the development of very promising IONPs for both capture and enrichment of bacteria has been envisioned.[31,32] Despite of the advantages of IONPs for bacteria capture and detection, separation of the remaining living bacteria is a major drawback in detoxification purposes like decontamination of water or targeted killing of bacteria localized inside a particular organ. Therefore, it is desired to envision nanoparticles for simultaneous capture and killing of bacteria from the system to be disinfected. For this purpose, surface of Ag@Fe$_2$O$_3$ yolk–shell nanoparticle conjugated with glucose *via* dopamine anchor have been developed.[33] Instead of glucose molecule conjugation, antibacterial drug can be more effective for bacteria separation and killing as reported earlier.[34] More than a decade ago, Kell *et al.* reported an extensive study on the multi-step preparation of a series of vancomycin modified silica encapsulated IONPs to isolate a variety of bacteria from aqueous solution.[35] This is understandable that silica encapsulation of IONPs favored easy functionalization required for anchoring vancomycin, but such practice generally reduces the magnetic property. Interestingly, vancomycin architecture and length of linker between nanoparticles and vancomycin showed significant effect on the magnetic confinement of pathogens. For comparison, commercially available 2.8 μm sized magnetic

Dynal beads were also used for modification with vancomycin. Though in neither case experimental evidence in support of magnetic property is provided. Recently, Chen *et al.*, and Zhang *et al.*, reported the potential of vancomycin modified magnetic nanoparticles for enhancing activity against *Clostridium difficile*, and *Staphylococcus aureus* and *Escherichia coli* respectively.[36,37] In the former report,[36] prostate specific membrane antigen (PSMA) was immobilized on oleic acid coated IONPs for conjugation with vancomycin. The mode of interaction of antigen with oleic acid coated IONPs is not clarified as weaker interaction may initiate leakage of immobilized vancomycin. In the latter one, Zhang and his coworkers developed a magnetic hybrid system comprising polyvinyl alcohol layered silica coated IONPs for entrapping vancomycin and the hybrid was further equipped with cell-penetrating haxapepetide using a multistep preparation method which is very laborious and time consuming.

In this work, antibacterial vancomycin conjugated IONPs synthesis *via* a facile multiple ligand–receptors interaction is reported for efficient separation and immediate killing of bacteria. In the first step oleic acid is displaced by hydrophilic dopamine (DOPA) molecules and then vancomycin is chemically bonded through amide linkage. The positive side of this facile synthetic route is that the process is easily scalable, environment-friendly, requires less hazardous chemicals and overall, the prepared antibacterial vancomycin conjugated IONPs would retain almost the same initial magnetic property and be biocompatible. Additionally, the hydrophilic vancomycin conjugation would improve water dispersibility and hence, would increase contact area between IONPs and bacteria, which is advantageous for enhanced antibacterial activity.

2. Experimental

2.1 Materials

Ferrous chloride tetrahydrate (FeCl$_2$·4H$_2$O), ferric chloride hexahydrate (FeCl$_3$·6H$_2$O), sodium hydroxide, dopamine hydrochloride (DOPA), 1-ethyl-3-(3-dimethylaminopropyl) carbodiimide (EDC) and *N*-hydroxysuccinimide (NHS) acid were obtained from Sigma Aldrich, USA and used as received. 25% ammonium hydroxide (NH$_4$OH), acetone, potassium phosphate monobasic and sodium phosphate dibasic were purchased from Acros organics, Belgium. Oleic acid was obtained from Fluka. Disinfectol and chloroform were obtained from Chemlab, Belgium. Vancomycin hydrochloride was obtained from Aldrich, Belgium. Three different bacterial strains namely *Bacillus subtilis*, *Streptococcus* and *Escherichia coli* were obtained from the Department of Biochemistry & Molecular Biology, Rajshahi University. The strains were preserved at 4 °C on agar slant and sub-cultured at 37 °C for 24 hours on nutrient broth media.

2.2 Methods

2.2.1 Preparation of oleic acid coated iron oxide (Fe$_3$O$_4$-OA) magnetic nanoparticles. Iron oxide, *i.e.*, magnetite (Fe$_3$O$_4$) nanoparticles were synthesized by co-precipitation method

using ferric (0.1 mole) and ferrous chloride (0.05 mole) salts at 2 : 1 molar ratio of Fe^{3+} : Fe^{2+}. Ferric and ferrous chloride were dissolved in 100 mL of water and heated to 80 °C followed by the addition of 15 mL of ammonium hydroxide, and the reaction was kept under mechanical stirring for 1 hour at ambient condition. Oleic acid (10 mL) was added to the reaction system to introduce a coating of oleic acid on magnetite nanoparticles denoted as Fe_3O_4-OA, and the reaction mixture was mechanically stirred for another 2 hours. Finally, the nanoparticles were purified by five times washing with water and ethanol, and the particles were dried and stored for further use.

2.2.2 Ligand exchange of Fe_3O_4-OA with dopamine (DOPA). The hydrophobic ligand, oleic acid, on Fe_3O_4-OA nanoparticles were replaced with hydrophilic dopamine molecules *via* a ligand exchange method with little modification of a previous report.[38] In brief, 50 mg of dried IONPs was dispersed in 5 mL of chloroform (10 mg mL^{-1}) using an ultrasonic bath for 5 minutes. 100 mg of DOPA was dissolved in 3 mL of degassed H_2O and then added to the IONPs suspension in chloroform. The mixture was sonicated for 45 minutes to complete the ligand exchange. The nanoparticles were then purified by magnetic decantation using water for five times washing to remove free dopamine.

2.2.3 Vancomycin (Van) conjugation on Fe_3O_4/DOPA nanoparticles. Vancomycin was conjugated on Fe_3O_4/DOPA nanoparticles *via* carbodiimide reaction. At first, three different concentrations, 5, 10 and 15 mg of vancomycin was prepared in 2 mL of phosphate buffer saline. Then, a mixture of 2 mL solution of 5 mM mL^{-1} of EDC and 5 mM mL^{-1} of NHS was added to the previous solutions to activate the carboxyl group of vancomycin. The activated vancomycin containing solution was added to a 6 mL suspension of 20 mg of Fe_3O_4/DOPA nanoparticles. The solution was adjusted at pH 6 and stirred overnight on a roller. The resulting Fe_3O_4/DOPA/Van nanoparticles were washed three times with water by using a magnet to remove unreacted EDC, NHS and vancomycin. The prepared Fe_3O_4/DOPA/Van nanoparticles were then redispersed in water and stored the suspension in a refrigerator at 4 °C for further experimentation and characterizations.

2.3 Characterization of the magnetic Fe_3O_4/DOPA/Van nanoparticles

The surface modification was confirmed with FTIR on a PerkinElmer Frontier FT-IR instrument in conjunction with a MKII Golden Gate set-up equipped with a diamond crystal. The size, shape and overall morphology of the NPs were evaluated with dynamic light scattering (DLS) technique and transmission electron microscopy (TEM). DLS was performed on an Autosizer 4800 Spectrometer from Malvern Instruments and TEM images were obtained with a Phillips CM120 microscope (CMEABG, University of Claude Bernard Lyon I, Villeurbanne, France). Magnetic behavior of the nanoparticles was investigated by vibrating sample magnetometer (VSM) at room temperature on the automatic bench of magnetic measurements at CNRS-IRCE Lyon, France. XRD measurements were carried out on a Bruker (Germany) D8 ADVANCE for the analysis of nanoparticle

structures. Powder samples were measured using Cu K$_\alpha$ radiation ($\lambda \approx 1.5406$ Å), AQ6 a tube voltage of 33 kV and a tube current of 45 mA. The intensities were measured at 2θ values from 10° to 90° at a continuous scan rate of 1° min^{-1} with a position-sensitive detector aperture at 25 °C. The obtained patterns were further processed by semi-quantitative phase analysis software to eliminate the noises to identify peaks.

2.4 Antibacterial activity study

The antibacterial activities of Fe_3O_4, Fe_3O_4/DOPA and Fe_3O_4/DOPA/Van nanoparticles were measured by a disc diffusion assay method. Three different microbial pathogens, Gram positive (*B. subtilis*, *S. aureus*) and Gram negative (*E. coli*) bacteria were tested in this study. Typically, 60 μL of bacterial solution was spread homogeneously on the surface of solid nutrient agar media in sterilized Petri dish. Sterile filter paper disks (10 mm) were then placed on the surface of cultured test bacteria at five different spots. Three different volumes *i.e.*, 5, 10 and 15 μL of Fe_3O_4/DOPA/Van nanoparticles suspension (2.5 mg mL^{-1}) were dropped on filter paper disk by a micropipette. 10 μL of vancomycin solution (0.002 mg mL^{-1}) was dropped for positive control and 10 μL phosphate buffered saline (PBS) was dropped for negative control experiment. In addition to that, bare Fe_3O_4 and dopamine modified Fe_3O_4 nanoparticles were also tested to compare with the Fe_3O_4/DOPA/Van nanoparticles. The plates were then placed in a refrigerator at 4 °C for 4 hours to permit sample diffusion and then incubated at 37 ± 1 °C for 24 hours to allow bacterial growth. Each experiment was carried out in triplicates and diameter (mm) of zone of inhibition across each filter paper disk was measured. Minimum inhibitory concentrations (MIC) of Fe_3O_4/DOPA/Van against three pathogens were also measured.
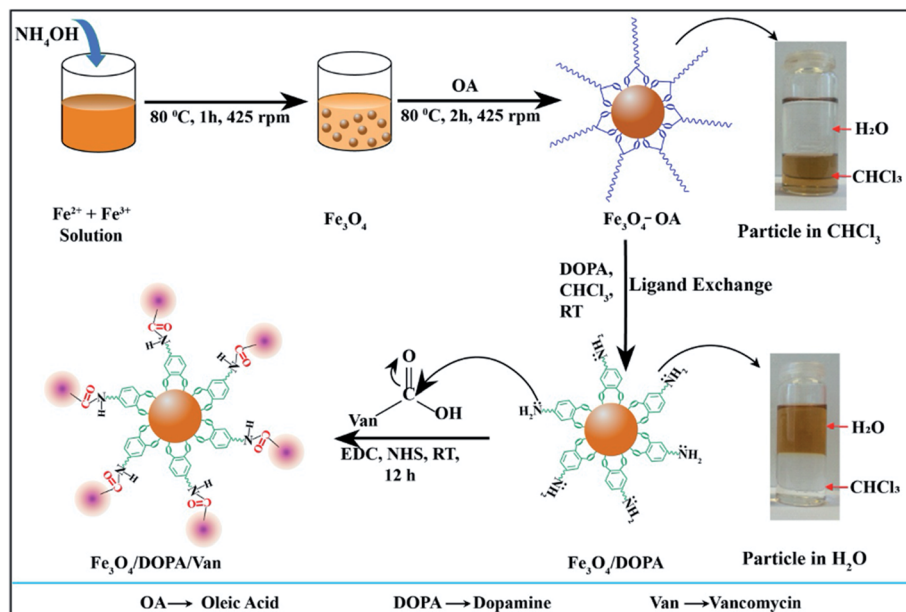
2.5 Bacteria separation test

The Gram positive and Gram-negative bacteria (concentration, 1×10^7 CFU per mL) were grown at 37 °C for 24 hours in broth media and then, optical microscopy images of the respective bacteria were taken. The Fe_3O_4/DOPA/Van nanoparticles were suspended in PBS, (0.01 M, pH 6–7 buffer) to prepare three different 2.65 mg mL^{-1}, 1.325 mg mL^{-1}, and 0.6625 mg mL^{-1} suspensions. Then 5 mL of each prepared suspensions was taken in test tube. 10 μL of each bacterial stain was added in each test tube and allow the mixture to stand for 10 minutes. Then quickly an external magnet was applied for the separation of bacteria attached to the nanoparticles. After washing twice, the magnetic nanoparticles were resuspended in PBS for optical microscopic analysis by N-800M (China).

3. Results and discussion

3.1 Characterization of Fe_3O_4-OA nanoparticles

The synthesis, surface modification and vancomycin conjugation of IONPs steps are schematically illustrated in Scheme 1. Hydrophobic Fe_3O_4-OA were synthesized by the coating of oleic acid on Fe_3O_4 and dispersible in organic solvent, *e.g.*, chloroform, as shown in the digital photograph (upper rightmost) of

Scheme 1 Schematic illustration for the synthesis, oleic acid coating, ligand exchange and vancomycin conjugation of iron oxide nanoparticles to obtain Fe_3O_4/DOPA/Van nanoparticles.
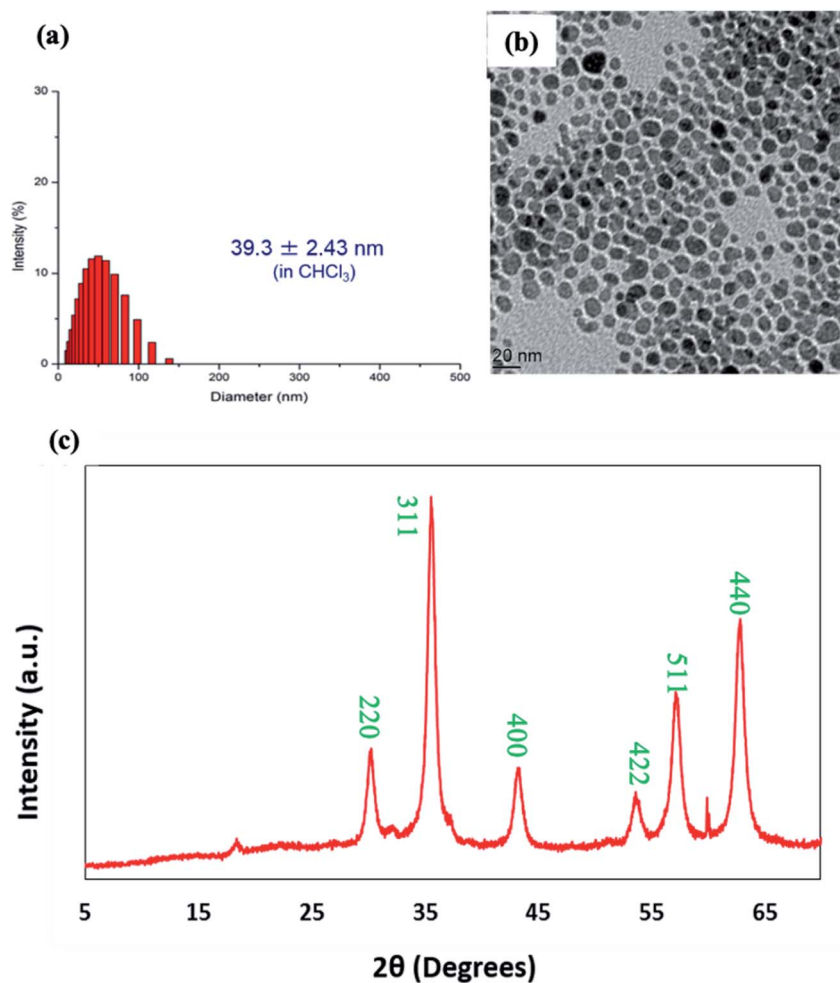

Fig. 1 (a) Size distribution measured by DLS, (b) TEM image and (c) XRD pattern of oleic acid coated iron oxide nanoparticles (Fe_3O_4-OA).
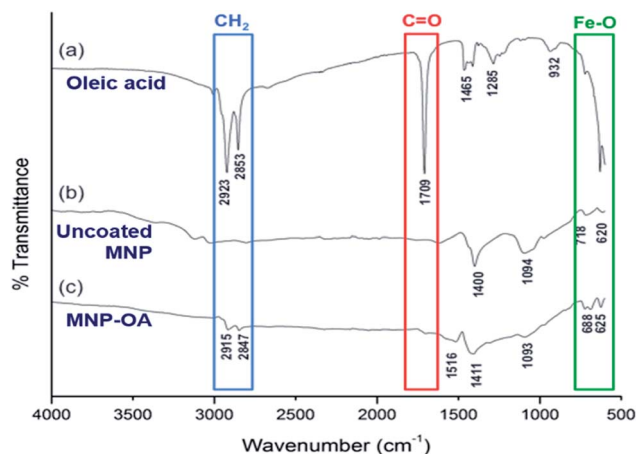
Fig. 2 FTIR spectra of (a) pure oleic acid, (b) uncoated magnetic nanoparticles (Fe_3O_4), and (c) oleic acid coated magnetic nanoparticles (Fe_3O_4-OA).
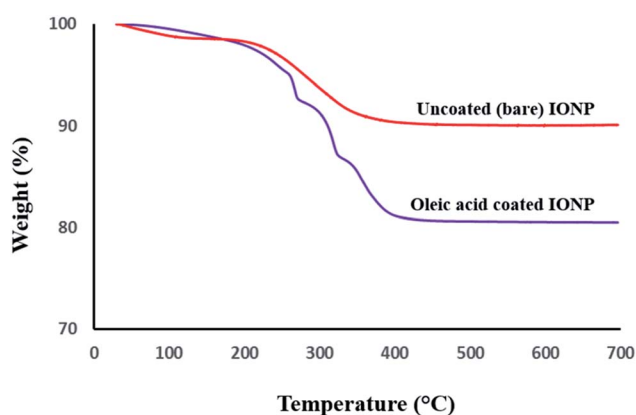

Fig. 3 Thermograms of the uncoated (upper curve) and oleic acid coated (lower curve) iron oxide magnetic nanoparticles.

Scheme 1. Oleic acid ligand exchange was performed to coat Fe_3O_4 with hydrophilic DOPA to obtain water dispersible hydrophilic Fe_3O_4-DOPA nanoparticles (lower rightmost). The

partitioning of nanoparticles from chloroform to water medium indicated successful ligand exchange from OA on Fe_3O_4-OA to DOPA on Fe_3O_4-DOPA nanoparticles. Amine functional group of DOPA was introduced on Fe_3O_4 to conjugate vancomycin *via* carbodiimide reaction using EDC and NHS.

The prepared Fe_3O_4-OA nanoparticles were readily dispersed in the chloroform. The suspension was stable for months in storage at 4 °C without noticeable sedimentation. Fig. 1a shows the size histogram obtained from DLS results indicating narrow size distribution. Though, the average hydrodynamic diameter of Fe_3O_4-OA nanoparticles was found to be 39.3 nm from DLS, but TEM image indicated the particle size in the range of 10–20 nm (Fig. 1b). Two-fold increase in particles size for DLS is due to hydrodynamic measurement and little aggregations of nanoparticles. This may be due in part to the presence of the oleic acid layer surrounding the particles.

The XRD pattern of Fe_3O_4-OA nanoparticles shown in Fig. 1c demonstrates the characteristic diffraction signal at two theta (2θ) value of 18° corresponding to amorphous segments of oleic acid coating. Sharp and strong diffraction signals at 2θ values of around 30.1°, 35.5°, 42.8°, 53.8°, 56.7° and 63.8° can be indexed to crystal planes of (220), (311), (400), (422), (511) and (440) respectively and matched well with the data base of crystalline iron oxide magnetite Fe_3O_4 nanoparticles.[39,40]

The surface coating of Fe_3O_4 with oleic acid was further studied and compared with pure oleic acid and uncoated Fe_3O_4 nanoparticles by FTIR spectra analysis (Fig. 2). The characteristic peaks at around 2920 and 2850 cm^{-1} were observed for asymmetrical and symmetrical stretching of –CH_2 present in both oleic acid (Fig. 2a) and oleic acid coated IONPs (Fig. 2c). Similar peaks were not present in uncoated nanoparticles (Fig. 1b), indicating the coating of oleic acid on the iron oxide nanoparticles. Owing to overlapping with –CH_2 stretching, no distinct –OH stretching peak for pure oleic acid was observed.[41] However, a peak at 932 cm^{-1} corresponds to the bending (out of plane) of –OH bond of carboxylic acid was visible. Additionally, the carboxylic C=O stretching represented by the sharp peak at 1709 cm^{-1} in oleic acid (Fig. 2a) is not present in IONPs-OA (Fig. 2c) due to the anchoring on surface of the nanoparticles. This result indicates that the IONPs are coated with a monolayer
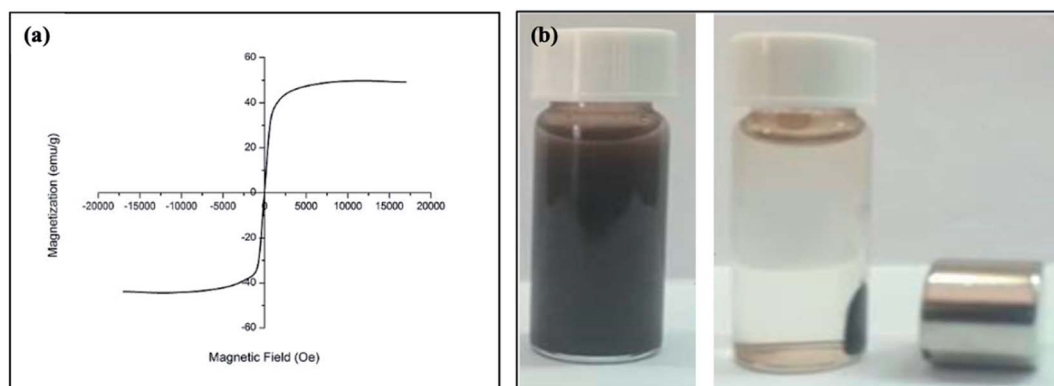

Fig. 4 (a) Magnetization value obtain from vibrating sample magnetometer (VSM) of Fe_3O_4 nanoparticles as a function of magnetic field strength (Oersted) and (b) digital photograph of oleic acid coated Fe_3O_4 nanoparticles suspension in absence and presence of a magnetic field.
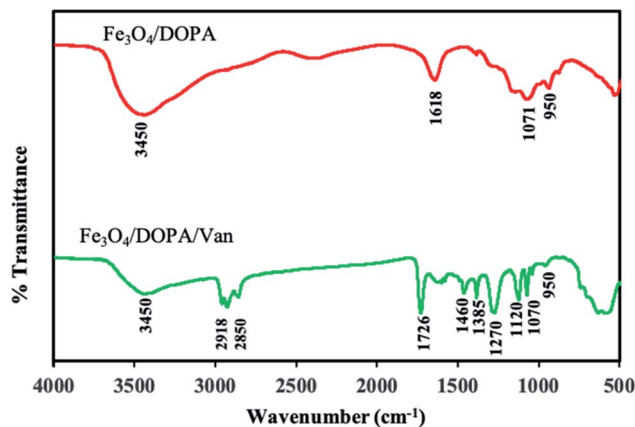
Fig. 5 FTIR spectra of (a) dopamine coated Fe_3O_4 nanoparticles after oleic acid replacement by ligand exchange method and (b) vancomycin conjugated magnetic $Fe_3O_4/DOPA/Van$ nanoparticles.

of oleic acid.[42] The disappearance of the above carboxylic stretching in MNP-OA is due to the anchoring of –COOH on the surface of nanoparticles. Besides, the absence of –OH peaks at 1516 and 1411 cm^{-1} attributed to the carboxylate (–COO^-) stretching indicating ligand binding on nanoparticle surface.[43,44] Lastly, the peaks at the lower wavenumbers, 620, 680, and 718 cm^{-1} represent the Fe–O stretching in both uncoated and oleic acid coated magnetic nanoparticles.[45]

TGA curves were acquired for further quantitative demonstration of surface coating with oleic acid on Fe_3O_4 nanoparticles (Fig. 3). The residual weight of uncoated magnetic nanoparticles is 96.4%. The 3.6% weight loss until 600 °C is attributed to adsorbed and chemisorbed water in uncoated Fe_3O_4. On the other hand, Fe_3O_4-OA nanoparticles showed a weight loss of ~18%. This higher weight loss corresponds to the pyrolysis of organic content (oleic acid), which can therefore

be attributed to surface coverage of Fe_3O_4. At temperatures 350 °C and above, the organic content was thermally decomposed, and the final weight (82%) reflects the inorganic iron oxide content of the sample.

Fig. 4a shows the hysteresis loops for oleic acid coated IONPs which were characterized using a VSM at room temperature. The VSM result demonstrated that the nanoparticles have superparamagnetic character with a saturation of magnetization of 42.5 emu g^{-1} at 300 K (Fig. 4a). The higher value of saturation of magnetization indicates an excellent magnetic response of IONPs to external magnetic field. The digital photograph of oleic acid coated IONPs suspended in chloroform demonstrates the well dispersibility in absence of magnetic field while the nanoparticles are accumulated easily by a magnet (Fig. 4b).

3.1.1. Conjugation of vancomycin to Fe_3O_4-OA nanoparticles. The FTIR spectra of dopamine coated $Fe_3O_4/DOPA$ and vancomycin conjugated $Fe_3O_4/DOPA/Van$ (Fig. 5) show broad absorption peaks at 3400 cm^{-1} corresponds to vibration of O–H stretching which might be merged with the stretching vibration of N–H bonds for later one. The absorption band at 1643 cm^{-1} was attributed to bending vibrations of N–H.[46,47] The intense three new bands for $Fe_3O_4/DOPA/Van$ at 1460, 1385 and 1270 cm^{-1}, which are absent in $Fe_3O_4/DOPA$, were originated from the vancomycin molecules. Most importantly, the detection of absorption band at 1726 cm^{-1} (C=O bond) confirmed the conjugation of vancomycin. The absorption bands at 580 and 520 cm^{-1} were related to Fe–O bonds in the tetrahedral and octahedral sites. The lower bond length of tetrahedral sites resulted higher stretching frequency i.e., the peak at 580 cm^{-1} corresponds to the intrinsic stretching vibrations of the Fe–O at the tetrahedral sites.[48,49] Another broad peak, which is due to merger of multiple peaks, at 1550–1650 cm^{-1} in $Fe_3O_4/DOPA/Van$ is attributed to the stretching vibration of amide I and amide II, also revealed vancomycin conjugation on IONPs.[50,51]

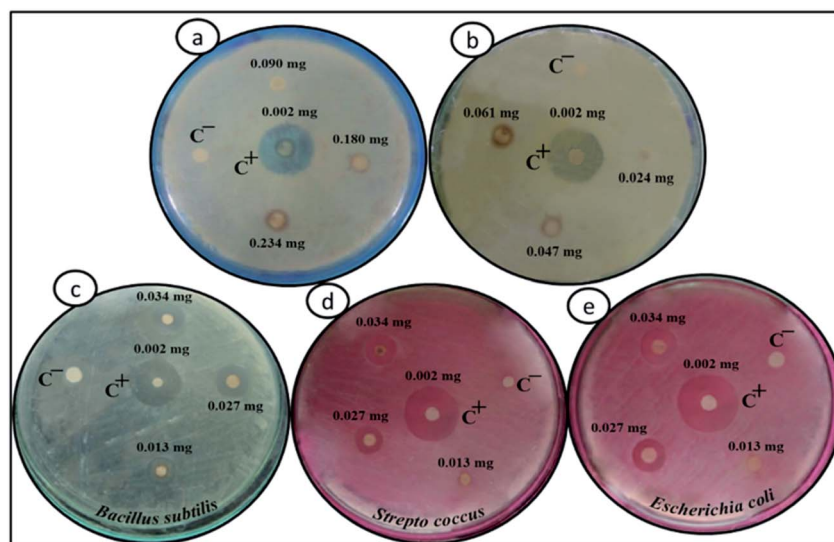**Fig. 6** Petri dish images for antibacterial test where (a) for oleic acid coated magnetite, Fe_3O_4–OA, (b) for $Fe_3O_4/DOPA$ and, (c) to (e) for different type of bacteria and different amount (mg per disk) of $Fe_3O_4/DOPA/Van$ nanoparticles. The central disk denoted as C^+ is for free vancomycin solution and the disk C^- is for $Fe_3O_4/DOPA$ as negative control. Rest of the disks are for concentration of $Fe_3O_4/DOPA/Van$ nanoparticles.
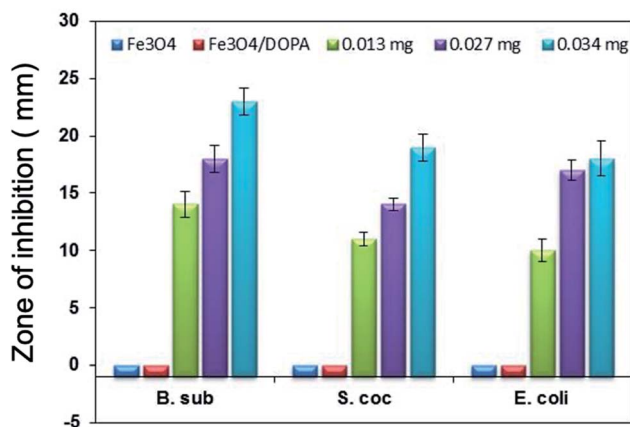
Fig. 7 Inhibition zone (mm) produced by different amount (mg/disk) of Fe$_3$O$_4$/DOPA/Van nanoparticles against three different bacteria, *B. subtilis*, *S. aureus* and *E. coli*.

3.1.2. Antibacterial studies of Fe$_3$O$_4$/DOPA/Van nanoparticles. Antibacterial activity of nanoparticles was initially investigated by comparing the growth inhibitory effects of two commonly used representative species, one is the Gram-positive bacteria, that is, *B. subtilis* (ATCC 6633), *Streptococcus* (ATCC 6538P) and the other is Gram-negative bacteria, *E. coli* (ATCC 35218), using an agar diffusion assay. The antibacterial properties of Fe$_3$O$_4$/DOPA/Van, Fe$_3$O$_4$/DOPA and Fe$_3$O$_4$-OA nanoparticles are shown in Fig. 6. It was found that bare Fe$_3$O$_4$ and Fe$_3$O$_4$/DOPA nanoparticles did not produce any zone of inhibition (ZI) which is like the previous report.[52] While Fe$_3$O$_4$/DOPA/Van nanoparticles conjugated with vancomycin show significant antibacterial property against both Gram positive (*B. subtilis* and *Streptococcus*) and Gram negative (*E. coli*) bacteria. Moreover, it is also observed (Fig. 7) that the ZI increases with the increase of Fe$_3$O$_4$/DOPA/Van concentration. Depending on the nature of bacteria, the inhibition zone in presence of Fe$_3$O$_4$/DOPA/Van nanoparticles changes between 10 to 23 mm. The nanoparticles revealed the minimum inhibitory concentration (MIC) at 0.010 mg mL^{-1} and, a maximum inhibition zone of 23 mm against *B. subtilis* for 0.034 mg per disc of nanoparticles. Whereas for the same nanoparticles, 18 mm zone of inhibition was found against *E. coli*. From the above results, the antibacterial property of Fe$_3$O$_4$/DOPA/Van nanoparticles is therefore
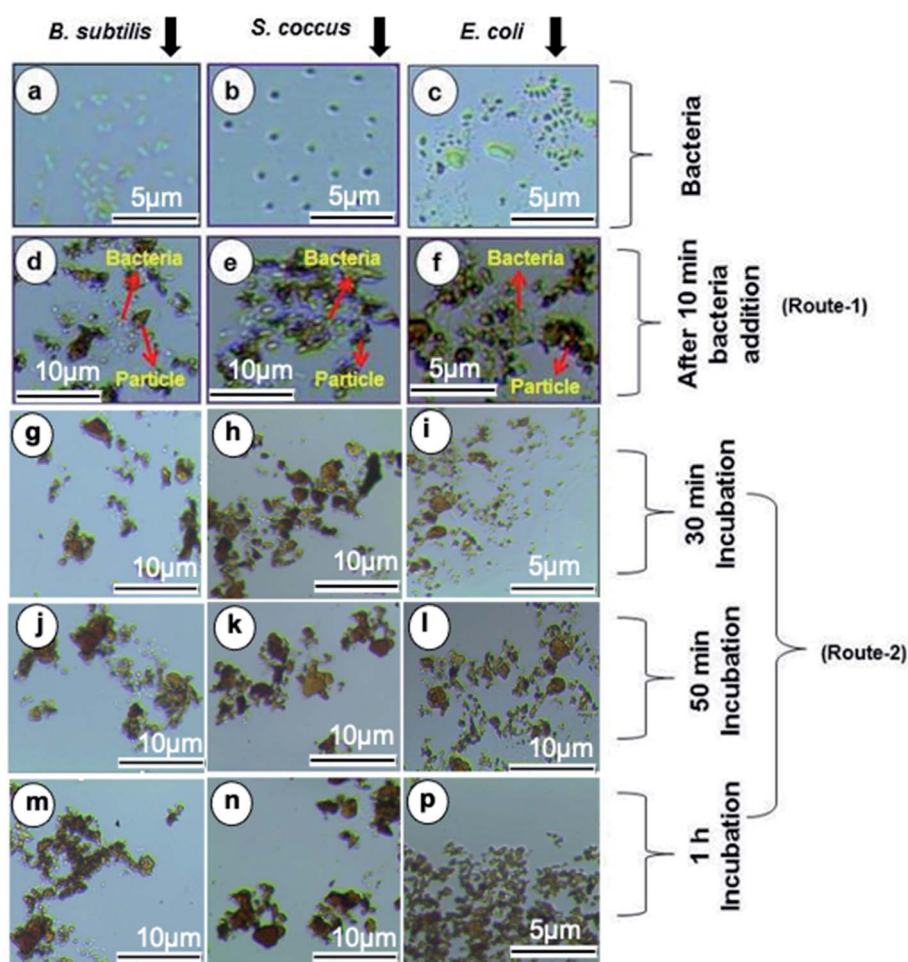

Fig. 8 Light microscopy images (a–c) for Gram-positive and Gram-negative bacteria before incubation with Fe$_3$O$_4$/DOPA/Van nanoparticles, and after incubation for different time intervals, minute (d–f) 10 (g–i) 30, (j–l) 50 and (m–p) 60. Routes 1 and 2 indicate without and with incubation time respectively (magnification × 40).

attributed to the conjugation of vancomycin on the surface of Fe$_3$O$_4$/DOPA nanoparticles.

3.1.3 Bacteria capture and killing by Fe$_3$O$_4$/DOPA/Van nanoparticles. Vancomycin kills bacteria by binding irreversibly to D-alanyl-D-alanine moieties of the *N*-acetylmuramic acid (NAM) and *N*-acetylglucosamine (NAG) peptides. This inhibits the synthesis and cross-linking of the NAM/NAG polymers that form the backbone of the bacteria cell wall. Unlike other nanoparticles coated with polymers, vancomycin functionalized magnetic nanoparticles are able to capture a broad range of bacteria *via* ligand–receptors interactions. More importantly, the glycopeptide antibiotic like vancomycin that is effective not only for capture but also for killing of bacteria by preventing formation of cell walls needed for bacteria survival. As described in the previous section, Fe$_3$O$_4$/DOPA nanoparticles did not show any bactericidal activity, therefore, only vancomycin functionalized Fe$_3$O$_4$/DOPA/Van IONPs have been employed for the bacteria capturing and killing of both Gram positive (*B. subtilis* and *S. aureus*) and Gram negative (*E. coli*) bacteria as models. Light microscopy images of different bacteria before and after incubation with nanoparticles for different time periods, are presented in Fig. 8. There is no observable change in shape, of rod-like *B. subtilis* and *E. coli* and

spherical *S. aureus*, bacterial species, that are well dispersed but not in aggregated form at before and after incubation. On the other hand, after 10 min of incubation a smaller number of bacteria is observed without any significant change in their shape (Fig. 8d–f) following attachment with Fe$_3$O$_4$/DOPA/Van nanoparticles and separation by an external magnet. This result indicates that Fe$_3$O$_4$/DOPA/Van nanoparticles can separate bacteria from the contaminated system. However, the aggregation of nanoparticles as observed might (Fig. 8g–p) has induced by the addition of bacteria agar medium to the suspension of nanoparticles. Expectedly, a prolonged incubation time of ≥30 minute induces more death of bacteria, leaving a few numbers of live bacteria in separation medium, which finally get attached to nanoparticles. Likewise, the number of bacteria evidently decreases with increase in incubation time (Fig. 8j–p). This is due to fact that the vancomycin modified magnetic nanoparticles have higher affinity towards living bacteria than that of the dead counterpart. This result might be because vancomycin not only inhibits cell growth but also ruptures cell wall, results in the breakage of hydrogen bonds and hence, ultimately lessens the bacteria attachment.

The separation and fate of bacteria after interaction with Fe$_3$O$_4$/DOPA/Van nanoparticles are schematically illustrated in

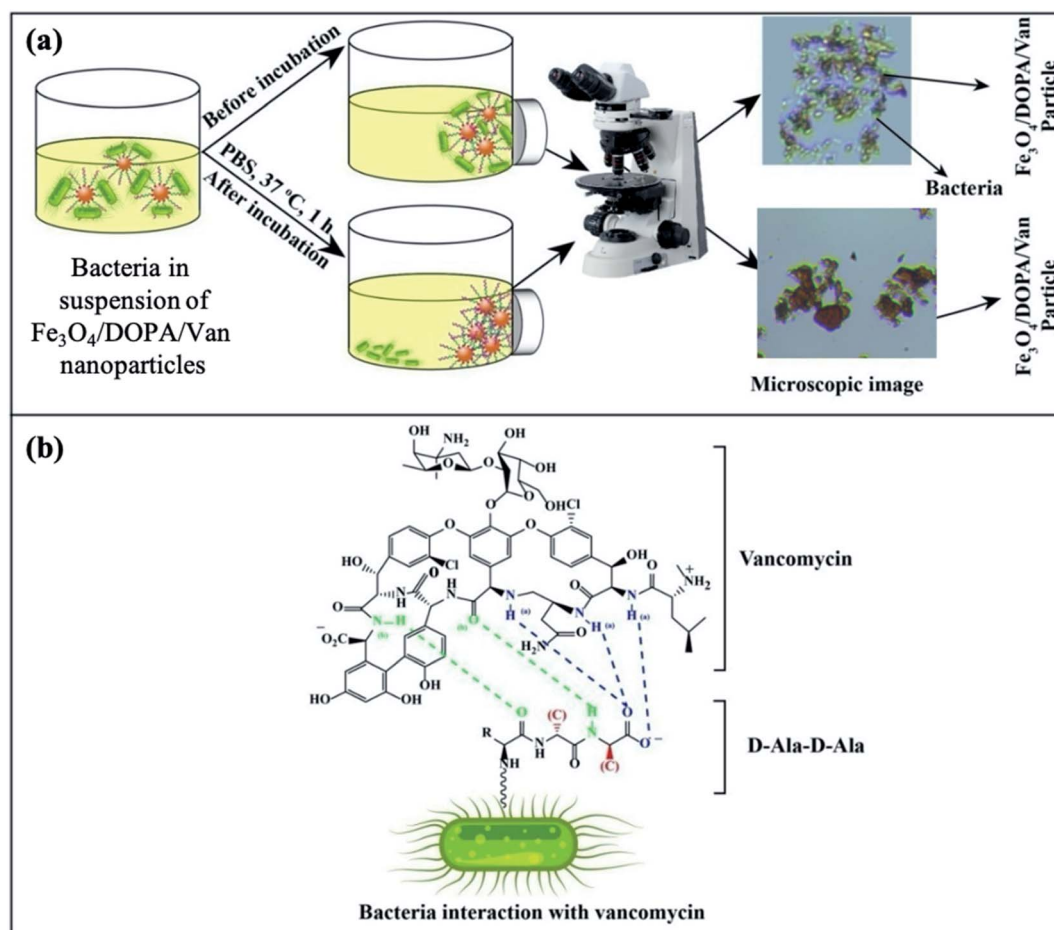**Fig. 9** (a) Schematic illustration for the separation of bacteria by vancomycin conjugated Fe$_3$O$_4$/DOPA/Van nanoparticles and (b) schematic representation of H-bonding interaction between vancomycin molecule and the D-alanyl-D-alanine dipeptide of bacterial surface.

Paper

the Fig. 9a which shows that how bacteria are attached and separated with the aid of Fe_3O_4/DOPA/Van nanoparticles just immediately after magnetic accumulation. This figure also illustrated that incubation of bacteria with Fe_3O_4/DOPA/Van nanoparticles for 1 hour leaves fewer number of dead bacteria due to longer contact with nanoparticles. Fig. 9b shows the molecular structure of vancomycin and glycopeptide of bacterial cell wall to elucidate how they interact each other. In the process, the vancomycin molecule containing various amino and amide groups forms hydrogen bonds with the terminal D-alanyl-D-alanine moieties of bacteria.[53,54] Therefore, bactericidal action of Fe_3O_4/DOPA/Van, is accounted primarily from inhibition of cell-wall biosynthesis due to the hydrogen bonding interaction as represented by dotted lines (Fig. 9b) and this ultimately leads to the death of cell.

4. Conclusion

Vancomycin conjugated with dopamine anchored iron oxide magnetite nanoparticles, Fe_3O_4/DOPA/Van, have been prepared and studied as antibacterial agent against both Gram positive and Gram-negative bacteria. A ligand exchange method facilitated easy transfer of highly crystalline hydrophobic magnetite (Fe_3O_4-OA) nanoparticles, that were prepared *via* coprecipitation method and oleic acid coating, into hydrophilic *i.e.*, water dispersible Fe_3O_4/DOPA nanoparticles using dopamine (DOPA) as a ligand. An important finding of this study is that dopamine, which provides amine (NH_2) functionality, played a key role, as evidenced by FTIR analysis, for the conjugation of vancomycin *via* carbodiimide chemistry. The Fe_3O_4/DOPA/Van nanoparticles not only showed a maximum 23 mm zone of inhibition but also killed those bacteria adhered to the nanoparticles within one hour. This result revealed that vancomycin conjugated Fe_3O_4/DOPA/Van nanoparticles showed high sensitivity towards bacteria. Further study to quantify the amount of conjugated vancomycin and their comparative study with the free counterpart, and quantitative efficiency of antibacterial effect are of future interests. The overall results suggests that Fe_3O_4/DOPA/Van nanoparticles synthesized here possessed enough affinity to the bacterial targets, conducive for killing bacteria in the dispersion media.

Authors contribution

The manuscript was written through the contributions of all authors and approved the final version of the manuscript by all authors. M. M. Rahman conceptualized and led the project. M. M. Rahman, M. S. Islam and M. M. Hossain contributed to funding collection. M. M. Rahman, H. Ahmad and A. Elaissari contributed to nanoparticle characterizations and data analysis. M. Rashid, A. Rabbi and T. Ara performed the antibacterial study.

Conflict of interest

The authors declare no conflicts of interest.

Acknowledgements

References

1 https://www.who.int/news-room/fact-sheets/detail/antimicrobial-resistance.

2 C. L. Ventola, *P. & T.*, 2015, **40**, 277–283.

3 D. A. Beauregard, D. H. Williams, M. N. Gwynn and D. J. Knowles, *Antimicrob. Agents Chemother.*, 1995, **39**, 781–785.

4 J. P. Mackay, U. Gerhard, D. A. Beauregard, D. H. Williams, M. S. Westwell and M. S. Searle, *J. Am. Chem. Soc.*, 1994, **116**, 4581–4590.

5 A. K. Schaefer, J. E. Melnyk, Z. He, F. D. Rosario and C. L. Grimes, in *Immunity and Inflammation in Health and Disease*, ed. S. Chatterjee, W. Jungraithmayr and D. Bagchi, Academic Press, 2018, ch. 14, pp. 175–187.

6 M. Ravelingien, S. Mullens, J. Luyten, M. D'Hondt, J. Boonen, B. D. Spiegeleer, T. Coenye, C. Vervaet and J. P. Remon, *Eur. J. Pharm. Biopharm.*, 2010, **76**, 366–370.

7 M. Mahmoudian and F. Ganji, *Prog. Biomater.*, 2017, **6**, 49–56.

8 S. Radin, J. T. Campbell, P. Ducheyne and J. M. Cuckler, *Biomaterials*, 1997, **18**, 777–782.

9 M. Theerasilp, W. Sungkarat and N. Nasongkla, *Bull. Mater. Sci.*, 2018, **41**(42).

10 S. Palanisamy and Y. M. Wang, *Dalton Trans.*, 2019, **48**, 9490–9515.

11 N. Gupta, C. Gupta, S. Sharma, B. Rathi, R. K. Sharma and H. B. Bohidar, *RSC Adv.*, 2016, **6**, 111099–111108.

12 L. F. E. Huerta-Núñez, G. C. Villanueva-Lopez, A. Morales-Guadarrama, S. Soto, J. Lopez, J. G. Silva, N. Perez-Vielma, E. Sacristan, M. E. Gudino-Zayas and C. A. Gonzalez, *J. Nanopart. Res.*, 2016, **18**, 284, DOI: 10.1007/s11051-016-3594-8.

13 M. M. Rahman and A. Elaissari, *Sep. Purif. Technol.*, 2011, **81**, 286–294.

14 W. Wu, Q. He and C. Jiang, *Nanoscale Res. Lett.*, 2008, **3**, 397, DOI: 10.1007/s11671-008-9174-9.

15 N. Zhu, H. Ji, P. Yu, J. Niu, M. U. Farooq, M. W. Akram, I. O. Udego, H. Li and X. Niu, *Nanomaterials*, 2018, **8**, 810, DOI: 10.3390/nano810081.

16 W. Wu, C. Z. Jiang and V. A. L. Roy, *Nanoscale*, 2016, **8**, 19421–19474.

17 M. M. Rahman, Y. Nahar, W. Ullah, A. Elaissari and H. Ahmad, *J. Polym. Res.*, 2015, **22**, 33, DOI: 10.1007/s10965-015-0673-y.

18 Q. Wang, J. Xiao, M. Zhan, X. He, W. Yuan and Y. Li, *Polym. Chem.*, 2021, **12**, 2132–2214.

19 Y. Nahar, M. A. Rahman, M. K. Hossain, M. K. Sharafat, M. R. Karim, A. Elaissari, B. Ochiai, H. Ahmad and M. M. Rahman, *Mater. Res. Express*, 2020, **7**, 016102, DOI: 10.1088/2053-1591/ab5be1.

20 J. Nayeem, M. A. A. Al-Bari, M. Mahiuddin, M. A. Rahman, O. T. Mefford, H. Ahmad and M. M. Rahman, *Colloids Surf., A*, 2021, **611**, DOI: 10.1016/j.colsurfa.2020.125857.

21 S. Badragheh, M. Zeeb, M. Reza and T. B. Olyai, *RSC Adv.*, 2018, **8**, 30550–30561.

22 J. Sherwood, Y. Xu, K. Lovas, Y. Qin and Y. Bao, *J. Magn. Magn. Mater.*, 2017, **427**, 220–224.

23 K. Wang, J. Fu, S. Wang, M. Gao, J. Zhu, Z. Wang and Q. Xu, *J. Colloid Interface Sci.*, 2018, **516**, 263–273.

24 M. Wu, D. Zhang, Y. Zeng, L. Wu, X. Liu and J. Liu, *Nanotechnology*, 2015, **26**, 115102, DOI: 10.1088/0957-4484/26/11/115102.

25 S. Mumtaz, L.-S. Wang, S. Z. Hussain, M. Abdullah, Z. Huma, Z. Iqbal, B. Creran, V. M. Rotello and I. Hussain, *Chem. Commun.*, 2017, **53**, 12306–12308.

26 N. Pimpha, N. Woramongkolchai, P. Sunintaboon and N. Saengkrit, *J. Cluster Sci.*, 2021, DOI: 10.1007/s10876-021-01990-0.

27 D. T. Nguyen, L. T. Pham, H. T. T. Le, M. X. Vu, H. T. M. Le, H. T. M. Le, N. H. Pham and L. T. Lu, *RSC Adv.*, 2018, **8**, 19707–19712.

28 J.-J. Lee, K. J. Jeong, M. Hashimoto, A. H. Kwon, A. Rwei, S. A. Shankarappa, J. H. Tsui and D. S. Kohane, *Nano Lett.*, 2014, **14**, 1–5.

29 C. Wang, H. Lin and C. Ye, *Front. Environ. Sci. Eng.*, 2016, **10**(6), 8.

30 R. Kadam, M. Maas and K. Rezwan, *ACS Appl. Bio Mater.*, 2019, **2**, 3520–3531.

31 D. Martínez-Matamoros, S. Castro-García, M. Balado, A. Matamoros-Veloza, M. Alonso Camargo-Valero, O. Cespedes, J. Rodríguez, M. L. Lemos and C. Jiménez, *RSC Adv.*, 2019, **9**, 13533–13542.

32 H. Gu, P.-L. Ho, K. W. T. Tsang, L. Wang and B. Xu, *J. Am. Chem. Soc.*, 2003, **125**, 15702–15703.

33 Z. Wei, Z. Zhou, M. Yang, C. Lin, Z. Zhao, D. Huang, Z. Chen and J. Gao, *J. Mater. Chem.*, 2011, **21**, 16344–16348.

34 H. Gu, K. Xu, C. Xu and B. Xu, *Chem. Commun.*, 2006, 941–949.

35 A. J. Kell, G. Stewart, S. Ryan, R. Peytavi, M. Boissinot, A. Huletsky, M. G. Bergeron and B. Simard, *ACS Nano*, 2008, **2**, 1777–1788.

36 Y.-H. Chen, T.-J. Li, B.-Y. Tsai, L.-K. Chen, Y.-H. Lai, M.-J. Li, C.-Y. Tsai, P.-J. Tsai and D.-B. Shieh, *Front. Microbiol.*, 2019, **10**, 1141, DOI: 10.3389/fmicb.2019.01141.

37 W. Zhang, R. Taheri-Ledari, Z. Hajizadeh, E. Zolfaghari, M. R. Ahghari, A. Maleki, M. R. Hamblin and Y. Tian, *Nanoscale*, 2020, **12**, 3855–3870.

38 Y. Liu, T. Chen, C. Wu, L. Qiu, R. Hu, J. Li, S. Cansiz, L. Zhang, C. Cui, G. Zhu, M. You, T. Zhang and W. Tan, *J. Am. Chem. Soc.*, 2014, **136**, 12552–12555.

39 S. S. U. Rahman, M. T. Qureshi, K. Sultana, W. Rehman, M. Y. Khan, M. H. Asif and M. Farooq, *Results Phys.*, 2017, **7**, 4451–4456.

40 U. Kurien, Z. Hu, H. Lee, A. P. Dastoor and P. A. Ariya, *RSC Adv.*, 2017, **7**, 45010–45021.

41 Y.-Y. Shi, B. Sun, Z. Zhou, Y.-T. Wu and M.-F. Zhu, *Prog. Nat. Sci.: Mater. Int.*, 2011, **21**, 447–454.

42 K. Yang, H. Peng, Y. Wen and N. Li, *Appl. Surf. Sci.*, 2010, **256**, 3093–3097.

43 J. D. Roo, F. V.-D. Broeck, K. D. Keukeleere, J. C. Martins, I. V. Driessche and Z. Hens, *J. Am. Chem. Soc.*, 2014, **136**, 9650–9657.

44 S. Mondini, M. Leonzino, C. Drago, A. M. Ferretti, S. Usseglio, D. Maggioni, P. Tornese, B. Chini and A. Ponti, *Langmuir*, 2015, **31**, 7381–7390.

45 H. Veeisi, A. Sedrpoushan, B. Maleki, M. Hekmati, M. Heidari and S. Hemmati, *Appl. Organomet. Chem.*, 2015, **29**, 834–839.

46 T. Touqeer, M. W. Mumtaz, H. Mukhtar, A. Irfan, S. Akram, A. Shabbir, U. Rashid, I. A. Nehdi and T. S. Y. Choong, *Energies*, 2020, **13**, 177, DOI: 10.3390/en13010177.

47 H.-M. Yang, H.-J. Lee, K.-S. Jang, C. W. Park, H. W. Yang, W. D. Heo and J.-D. Kim, *J. Mater. Chem.*, 2009, **19**, 4566–4574.

48 Y. Xu, J. Sherwood, Y. Qin, R. A. Holler and Y. Bao, *Nanoscale*, 2015, **7**, 12641–12649.

49 J. Sherwood, Y. Xu, K. Lovas, Y. Qin and J. Yuping Bao, *Mag. Mag. Mater*, 2017, **427**, 220–224.

50 H.-M. Yang, H. J. Lee, K.-S. Jang, C. W. Park, H. W. Yang, W. D. Heo and J.-D. Kim, *J. Mater. Chem.*, 2009, **19**, 4566–4574.

51 H. Chen, T. Chen, J. Hu and C. Wang, *Colloids Surf., A*, 2005, **268**, 24–29.

52 D. Liu, L. Ma, L. Liu, L. Wang, Y. Liu, Q. Jia, Q. Guo, G. Zhang and J. Zhou, *ACS Appl. Mater. Interfaces*, 2016, **8**, 24455–24462.

53 B. K. Hubbard and C. T. Walsh, *Angew. Chem., Int. Ed.*, 2003, **42**, 730–765.

54 C. T. Walsh, *Science*, 1999, **284**, 442–443.